FORM 2

THE PATENTS ACT 1970

39 of 1970

&

The Patent Rules 2003

COMPLETE SPECIFICATION

(See sections 10 & rule 13)

1. TITLE OF THE INVENTION

Sn-ALLOY NANOPARTICLE CARBON ONE-DIMENSIONAL ASSEMBLIES FOR RECHARGEABLE BATTERIES

2. APPLICANTS (S)

NAME	**NATIONALITY**	ADDRESS
Indian Institute of Science	**Indian**	**Solid State and Structural Chemistry Unit, Indian Institute of Science Bangalore, Karnataka 560012, India**

3. PREAMBLE TO THE DESCRIPTION

COMPLETE

The following specification particularly describes the invention and the manner in which it is to be performed

COMPLETE SPECIFICATION

TITLE OF THE INVENTION

Sn-Alloy Nanoparticle Carbon One-Dimensional Assemblies for Rechargeable Batteries

CROSS REFERENCE TO RELATED APPLICATION

[0001] This application claims priority from the Provisional Application No. 4589/CHE/2013 filed on 10.10.2013.

FIELD OF THE INVENTION

[0002] The present invention relates to an integrated method for synthesis of Sn-Alloy Nanoparticle Carbon Electrode System in one dimensional configuration. The present invention also relates to use of the Sn-Alloy nanoparticle carbon electrode as an anode active material in a secondary battery.

BACKGROUND OF THE INVENTION

[0003] Energy storage systems, such as, lithium-ion batteries, are widely used as portable power sources for consumer electronic devices, in electric vehicles, in electric power grids because of their high energy density and flexible design. Concerns over the safety of earlier lithium secondary batteries led to the development of lithium-ion secondary batteries, in which pure lithium metal sheet or film was replaced by carbonaceous materials as the anode.

[0004] Lithium-ion batteries are rechargeable batteries in which lithium ions (Li^+) transfer between the anode and cathode during discharging and from cathode to anode during charging. Lithium-ion batteries, the most popular power sources on the market for portable electronic devices, can be used for electric vehicles if energy density can be enhanced. In the last decade, extensive efforts have been made to increase the capacity of anodes by replacing the currently used graphite with Si or Sn.

[0005] An amorphous carbon phase alone tends to exhibit a low electrical conductivity (high charge transfer resistance) and hence a high polarization or internal power loss. Conventional amorphous carbon-based anode materials also tend to give rise to a high irreversible capacity.

[0006] In addition to carbon- or graphite-based anode materials, other inorganic materials that have been evaluated for potential anode applications include metal oxides, metal nitrides, metal sulfides, and a range of metals, metal alloys, and intermetallic compounds that can accommodate lithium atoms or ions.

[0007] However, for the anodes composed of these materials especially ones storing via alloying reactions, degradation (pulverization) proceeds with the progress of charging and discharging cycles due to expansion and contraction of the anode during absorption and desorption of lithium ions. The expansion and contraction also tend to result in reduction in or loss of particle-to-particle contacts or contacts between the anode and its current collector. These adverse effects result in a significantly shortened charge-discharge cycle life.

[0008] To overcome the problems associated with such mechanical degradation, composites composed of small electrochemically active particles supported with less active or non-active matrices have been proposed for use as an anode material. Examples of these active particles are Si, Sn, and SnO_2. However, most of prior art composite electrodes have deficiencies in some

ways, for example, in most cases, less than satisfactory reversible capacity at varying currents, poor cycling stability, large irreversible capacity loss, ineffectiveness in reducing the internal stress or strain during the lithium ion insertion and extraction steps, and/or undesirable side effects.

[0009] Tin and tin-based compounds store much higher amounts of lithium, an order higher than commercial graphite anode. A fairly high overall cell potential of more than 3 V can be delivered when tin and tin-based compounds are used in conjunction with a layered or a spinel cathode. However, practical use of Sn/Sn-based compounds as anode in rechargeable batteries has been hindered by its large initial irreversible capacity loss and severe capacity fading upon successive cycling.

[0010] Various approaches have been employed to improve the battery performance especially using Sn-alloy particle and carbon electrodes. All approaches generally target to control the volume expansion or contraction during the alloying and de-alloying reaction and improvement of the electronic conductivity of Sn-alloy particle which can be achieved by embedding them in a matrix that can buffer or constrain the volume changes during electrochemical cycling.

[0011] It is believed that a carefully drafted Sn-alloy and carbon composite on the nanoscale may solve the poor cyclability of the tin electrodes.

[0012] Techniques for the production of nanoparticles include (a) chemical and (b) physical methods. Physical methods such as gas-phase condensation, spray pyrolysis, laser ablation and plasma synthesis involve energetic process conditions that rapidly lead to large amorphous aggregated particles or vitrified non-porous pigment-grade particles. For example, vapor phase nucleation produces crystalline non-porous particles (US 5,358,695) while flame synthesis with advanced controls like size control by charging, described by US Patent No. 5,861,132, permits

to produce particles of about 13 nm, but the anatase TiO_2 obtained contains undesirable rutile impurities that have a low conductivity.

[0013] Furthermore, there is an urgent need to develop scalable processes for safe, economical and environmentally friendly production of these improved porous materials and electrodes.

[0014] Bo-Ok Jang et. al. (2013, Journal of Alloys and Compounds) discloses Co–Sn alloy embedded carbon nanofiber (Co–Sn/CNF) composites functioning as anode materials in lithium ion batteries.

[0015] US Patent Publication US20130126794 discloses a method for preparing a carbon nanofiber in which a nano-sized metal oxide or an intermetallic compound dispersed is described.

[0016] Xifei Li et al (2013, Electrochimica Acta) discloses nanosized M_xSn (M = Ni, Fe, and Cr) alloys which were encapsulated in amorphous carbon nanotubes (ACNTs) creating hybrid anode heterostructures.

[0017] The most successful method for improving cycling stability is to form a C/Sn nanocomposite. Electrospinning has been used to synthesize C/Sn composites by dispersing Sn nanoparticles in porous multichannel carbon microtubes or bamboo-like hollow carbon nanofibers. The porous C/Sn composite materials have two-fold advantages: the porous structure of the C/Sn composites provides additional space to accommodate the volume variation, reducing the tin particle pulverization; and the porous carbon matrix can avoid the oxidation and aggregation of Sn nanoparticles and provides a continuous electron pathway. However, the electrospinning synthesis approach still faces challenges to control the morphology and component ratio of C/Sn.

[0018] Hence, there is a need in the art to develop an integrated synthetic method to assemble Sn-alloy nanoparticles with one-dimensional carbon structures to overcome structural instability of Sn and control Sn aggregation during long battery cycling. Such synthetic method must also optimize drastic volume changes occurring during successive metal uptake and removal that often leads to electrode disintegration and reduced battery life. Such integrated synthetic method must also have a uniform morphology. The present invention satisfies these needs, as well as others, and generally overcomes the deficiencies found in the background art.

[0019] All publications herein are incorporated by reference to the same extent as if each individual publication or patent application were specifically and individually indicated to be incorporated by reference. Where a definition or use of a term in an incorporated reference is inconsistent or contrary to the definition of that term provided herein, the definition of that term provided herein applies and the definition of that term in the reference does not apply.

OBJECTS OF THE INVENTION

[0020] It is a main object of the invention to provide an integrated method for synthesis of Sn-alloy nanoparticle assembly inside one-dimensional carbon structures.

[0021] It is another object of the invention to provide an integrated method for synthesis of Sn-alloy nanoparticle assembly inside one-dimensional porous carbon structures using an electrochemical technique coupled with an optimized heat sintering protocol.

[0022] It is yet another object of the invention to provide a Sn-alloy nanoparticle carbon electrode system with stable cyclability and functionality.

[0023] It is another object of the invention to provide a Sn-alloy nanoparticle carbon electrode which has uniform morphology.

[0024] It is another object of the invention to provide an integrated method for synthesis of Sn-alloy nanoparticle carbon electrode for use as an anode active material in a secondary battery such as lithium rechargeable battery.

[0025] It is another object of the invention to provide a Sn-alloy nanoparticle carbon electrode system which is compatible with various battery chemistries, for example lithium, sodium, metal-air systems, and the like.

[0026] It is a further object of the invention to provide an active Sn-alloy nanoparticle carbon electrode material with desired lithium storage capacity.

[0027] It is yet another object of the invention to provide a Sn-alloy nanoparticle carbon electrode system wherein no carbon additive is necessary for assembly of battery electrodes.

[0028] Other objects of the inventions will be apparent from the description of the invention herein below.

SUMMARY OF THE INVENTION

[0029] The present invention provides an integrated method for synthesis of Sn-alloy nanoparticle assembly embedded inside one dimensional porous carbon nanofibres comprising the steps of:

(i) electrospinning a precursor to produce nanofibre, the precursor comprising of polymer and Sn-X compositions; and

(ii) heat sintering and carbonization of the nanofibre to obtain the Sn-alloy nanoparticle assembly embedded inside the one dimensional porous carbon nanofibres;

wherein X is an element and the molar composition of Sn and element is 1:1; and the Sn-alloy nanoparticle assembly embedded inside one dimensional porous carbon nanofibres acts as an electrode.

[0030] In an embodiment of the present invention, the polymer is selected from the group comprising of polyacrylonitrile (PAN), polyvinyl alcohol (PVA), polyethylene oxide (PEO), and polyvinyl pyridine (PVP), poly(methyl) methacrylate (PMMA).

[0031] In another embodiment of the present invention, the element is selected from the group comprising antimony (Sb), cobalt (Co), iron (Fe), Ge (germanium), nickel (Ni), copper (Cu), or the combination thereof.

[0032] The Sn-alloy nanoparticle assembly inside one dimensional porous carbon structures prepared by the integrated method of the present invention has excellent charge or discharge rate capability and produces cells with high capacity and extended cycle performance.

[0033] In an embodiment of the present invention, interparticle distance inside Sn-alloy nanoparticles ranges from 10 to 30 nm and the interparticle distance in contact with carbon fibers is about 150 ± 50 nm.

[0034] In another embodiment of the present invention, Sn-alloy nanoparticle assembly arranged inside one-dimensional porous carbon structures is used as an electrode system in rechargeable batteries.

[0035] In yet another embodiment of the present invention, a Sn-alloy carbon nanofiber is used as an anode in various battery chemistries such as lithium, sodium, metal-air systems and the like.

[0036] In a still another embodiment of the present invention, one dimensional porous carbon structures enhances mechanical stability of particles and controls in-situ particle aggregation during successive battery cycling.

[0037] In a still another embodiment of the present invention, battery performance is optimized by the uniform distribution of the pores and particles in a one-dimensional network.

[0038] In a still another embodiment of the present invention, Sn-alloy carbon nanofiber does not require use of carbon additive which is otherwise necessary for assembly of battery electrodes. Furthermore, no additives are required to be added to liquid electrolyte for establishment of a stable electrode-electrolyte interface.

[0039] In a still another embodiment of the present invention, Sn-alloy carbon nanofiber is compatible with wide range of electrolytes like liquid, soft matter electrolytes and the like.

[0040] A secondary battery using Sn-alloy nanoparticle assembly arranged inside one-dimensional porous carbon structures prepared by the integrated method of the present invention is also disclosed wherein the secondary battery may be lithium, sodium, metal air systems and the like.

BRIEF DESCRIPTION OF THE DRAWINGS

[0041] These and other features, aspects and advantages of the invention will become better understood when the following detailed description is read with reference to the accompanying drawings wherein the drawings are with respect to an embodiment wherein the Sn alloy is SnSb, wherein:

[0042] **Figure 1** illustrates XRD patterns of SnSb-C nanofibers carbonized at different temperatures

[0043] **Figure 2** illustrates FTIR spectra of (a) PAN, (b) as-spun nanofibers stabilized at 200 < T < 300 ^{0}C in air, and (c) carbonized under reducing atmosphere for several hours.

[0044] **Figure 3** illustrates FESEM images of SnSb-C nanofibers obtained under varying electrochemical conditions optimized using the parameters as in table 1.

[0045] **Figure 4** illustrates SEM images of optimized SnSb-C fiber (table 1) composites following calcination at different magnifications used in the LIBs.

[0046] **Figure 5** illustrates TEM images of optimized and calcined SnSb-C fibers (table 1) composites used for the battery studies. Inset: shows the selected area diffraction (SAED) pattern of SnSb-C fibers.

[0047] **Figure 6** illustrates Raman spectrum of the SnSb-C nanocomposite.

[0048] **Figure 7** illustrates Thermogravimetric analysis (TGA) of the SnSb-C fibers.

[0049] **Figure 8** illustrates Cyclic voltammograms for the 1st to 5th cycle for the porous (a) Sb-C, (b) Sn-C and (c) SnSb-C fibers nanocomposite.

[0050] **Figure 9** illustrates Galvanostatic charge–discharge profile of SnSb-C composite.

[0051] **Figure 10** illustrates Specific capacity versus cycle number of Sb-C, Sn-C and SnSb-C composite.

[0052] **Figure 11** illustrates Rate capability of SnSb-C composite at different currents.

[0053] **Figure 12** illustrates the Electrochemical Impedance Spectroscopy(EIS) Measurements: 12.1 depicts the ac-impedance spectra of SnSb-C composite electrode before and after cycling and 12.2 depicts the Equivalent Circuit Model to analyze the impedance spectra.

DETAILED DESCRIPTION OF THE INVENTION

[0054] Nanotechnology is the manipulation of matter at an atomic and molecular scale and is a diverse field involving many different structures, techniques and potential applications. Of them, one structure is a nanofiber, which generally has a diameter of less than a few microns and can be of various lengths.

[0055] Carbon nanofibers, like other one-dimensional nanostructures such as nanowires, nanotubes, and molecular wires, have been received increasing attention because of their high length-to-diameter ratio. This is due to their potential applications in nanocomposites, templates for nanotubes, filters, rechargeable batteries, supercapacitors, bottom–up assembly in nanoelectronics and photonics, and so forth.

[0056] Carbon nanofibers can be produced by traditional vapour growth method or plasma enhanced chemical vapour depositing method, which was developed at the beginning of this century. Carbon nanofibers can also be produced by stabilizing, carbonizing, and activating electrospun precursors. The rapidly developing technique of electrospinning provides a straightforward and cost-effective approach to produce fibers with diameters ranging from sub-microns to nanometers. Electrospinning is a simple and versatile method for generating ultrathin fibers from a rich variety of materials that include polymers, composites and ceramics. This non-mechanical, electrostatic technique involves the use of a high voltage electrostatic field to charge the surface of a polymer solution droplet and thus to induce the ejection of a liquid jet through a spinneret. Sintering is the process of making objects from powder, by heating the material in a furnace below its melting point so that bonding takes place by diffusion of atoms. This leads to individual powder particles adhering to each other in a dense compact.

[0057] Synthesis of Sn porous nanostructures eliminates drawback of irreversible capacity loss and severe capacity fading upon successive cycling. Hollow or void space created can suitably accommodate volume expansion taking place during charge-discharge process. Rather than storing directly in Sn, an effective approach towards optimization of drastic volume changes which can be achieved by storing lithium in compounds where Sn has alloyed with another element (for example binary, ternary). This strategy becomes even more effective when alloy particles are arranged inside a carbon matrix. An advantage of Sn-alloys over Sn or Sn-based compounds is that the Sn in the alloy stores lesser amount of lithium. An alloying element(s) also participate in reversible lithium storage. As a whole, the alloy exhibits a stepwise lithium insertion mechanism in to the components (that is Sn and X) which reduces volume changes (in Sn) and improve a mechanical stability of electrodes. This leads to better electrochemical properties than a single phase Sn.

[0058] The embodiments herein and the various features and advantageous details thereof are explained more fully with reference to the non-limiting embodiments that are illustrated in the accompanying figures and detailed in the following description.

[0059] The present invention provides an integrated method for synthesis of Sn-alloy nanoparticle assembly inside one dimensional porous carbon structures comprising the steps of:

(i) electrospinning a precursor to produce nanofibre, the precursor comprising of polymer and Sn-X compositions; and

(ii) heat sintering and carbonization of the nanofibre to obtain the Sn- alloy nanoparticle assembly inside the one dimensional porous carbon nanofibres;

wherein X is an element and the molar composition of Sn and element is 1:1; and the Sn-alloy nanoparticle assembly embedded inside one dimensional porous carbon nanofibres acts as an electrode.

[0060] In an embodiment of the present invention, the polymer is selected from the group comprising polyacrylonitrile (PAN), polyvinyl alcohol (PVA), polyethylene oxide (PEO), and polyvinyl pyridine (PVP), and poly(methyl)methacrylate (PMMA).

[0061] In another embodiment of the present invention, the element is selected from the group comprising antimony (Sb), cobalt (Co), iron (Fe), Ge (germanium), nickel (Ni), copper (Cu), or the combination thereof.

[0062] The Sn-alloy nanoparticle assembly inside one dimensional porous carbon structures manufactured by the integrated method as claimed in the present invention has excellent charge or discharge rate capability and produces cells with high capacity and extended cycle performance.

[0063] In an embodiment of the present invention, the interparticle distance inside Sn-alloy nanoparticles ranges from 10 to 30 nm and the interparticle distance in contact with carbon fibers is about 150 ± 50 nm.

[0064] In another embodiment of the present invention, Sn-alloy nanoparticle assembly arranged inside one-dimensional porous carbon structures is used as an electrode system in rechargeable batteries.

[0065] In yet another embodiment of the present invention, a Sn-alloy carbon nanofiber is used as an anode in various battery chemistries such as lithium, sodium, metal-air systems and the like.

[0066] In a still another embodiment of the present invention, one dimensional porous carbon structures enhances mechanical stability of particles and controls in-situ particle aggregation during successive battery cycling.

[0067] In a still another embodiment of the present invention, battery performance is optimized by the uniform distribution of the pores and particles in a one-dimensional network.

[0068] In a still another embodiment of the present invention, Sn-alloy carbon nanofiber does not require use of carbon additive which is otherwise necessary for assembly of battery electrodes. Furthermore, no additives are required to be added to liquid electrolyte for establishment of a stable electrode-electrolyte interface.

[0069] In still another embodiment of the present invention, Sn-alloy carbon nanofiber is compatible with wide range of electrolytes like liquid, soft matter electrolytes and the like.

[0070] A secondary battery using Sn-alloy nanoparticle assembly arranged inside one-dimensional porous carbon structures prepared by the integrated method of the present invention is also disclosed wherein the secondary battery may be lithium, sodium, metal air systems and the like.

[0071] Additional embodiments and features of the present invention will be apparent to one of ordinary skill in art based upon description provided herein and the examples provided below. However, the examples and the accompanying figures should not be construed to limit the scope of the present invention.

EXAMPLES

[0072] The embodiments herein and the various features and advantageous details thereof are explained more fully with reference to the non-limiting embodiments that are illustrated in the

accompanying figures and detailed in the following description. Descriptions of well-known components and processing techniques are omitted so as to not unnecessarily obscure the embodiments herein. The examples used herein are intended merely to facilitate an understanding of ways in which the embodiments herein may be practiced and to further enable those of skill in the art to practice the embodiments herein. Accordingly, the examples should not be construed as limiting the scope of the embodiments herein.

[0074] The preparation, structural characterization and battery performance of a binary alloy (SnSb) nanoparticle in porous carbon fibers is given below:

Example 1

Preparation of SnSb-C Fibers

[0075] The precursor solution for electrospinning was prepared by dissolving 0.4 g of a polyacrylonitrile (PAN, MW= 150000, Aldrich) in 4 ml of dimethylformamide (DMF) solvent and heated at around 70 ^{o}C by stirring overnight. The solution of 1:1 molar ratio of $SnCl_2$ and $SbCl_3$ were slowly added to the PAN solution and vigorously stirred for another 8-12 h to obtain the precursor for electrospinning. As-prepared precursor was loaded into 5 ml syringe needle. The flow rate of the solution was kept at 0.5-0.8 ml h^{-1} and the metallic needle was connected to a high voltage power supply (Physics equipments Co. Chennai India). 10-18 kV was applied between the needle and a grounded alumina foil, which was used to collect the nanofibrous mat. The distance between the needle and collector was 15 cm. Following the electrospinning process, a white color of $SnCl_2$, $SbCl_3$ and PAN composite mat was obtained on aluminum collector. The as-collected electrospun fibrous mats were stabilized in air (oxygen) at 280 °C for 3 h. Subsequently, the mats were heat sintered and carbonized in a tube furnace at 600-800 °C in

Ar/H_2 (95 vol%/ 5 vol%) for 3-5 h to obtain the SnSb nano particles embedded in graphitic carbon nanofibers. The heating rate was kept at 5-10 ºC/min.

Example 2

Physical Characterization of SnSb-C Fibers

[0076] The structure and crystallographic phase identification of various samples were investigated using powder X-ray diffraction (XRD, Philips). The Powder XRD patterns of SnSb-C fibers at different annealing temperatures are shown in Figure 1. At 700 °C all reflections correspond to the β-SnSb phase (ICDD #33 - 0118) which belongs to the space group R-3m (166). The lattice parameters of *β*-SnSb phase are a= b= 4.3251 Å and c= 5.3376 Å in a rhombohedral structure. There were no peaks arising out of the remnant impurities. For samples sintered at temperatures > 700 °C, separate peaks belonging to Sn start appearing. As a result of this, samples sintered at 700 °C were selected for all studies. In order to examine the nature of chemical bond formation in the nano fibre samples, FT-IR (Fourier Transform Infrared) measurement was done using FTIR Spectrometer Spectrum 1000. FT-IR spectra were obtained as shown in Figure 2. All prominent bands of the PAN structure at 2939, 2243, 1454, and 1360 cm^{-1} assigned to ν_{CH} (stretch) in CH_2, $\nu_{C\equiv N}$ (stretch) in CN, δ_{CH} in CH_2, and δ_{CH} in CH, respectively were observed for the as prepared PAN fibers. After stabilization at 280 °C, there was significant change in the structure because the two dominant peaks at 2939 cm^{-1} and 2240 cm^{-1} almost disappeared. Appearance of the peak at 1590 cm^{-1} is due to a mix of C=C, C=N and =C-H and peak at 1350–1380 cm^{-1} is due to the CH_3 group. Following sintering at 700 °C for 3 h under Ar/H_2 (95 vol%/ 5 vol%), no PAN peak was observed suggesting the formation of SnSb-C nanofibers.

[0077] The surface morphologies of the samples were investigated by Field Emission Scanning Electron Microscopy (FE-SEM, JEOL JSM - 5600LV) and Transmission Electron Microscopy (TEM, FEI Technai F30).

[0078] Figure 3 shows some of the different morphologies obtained as a result of selection of different electrospinning conditions as given in Table 1. The applied electric voltage was observed to have a significant effect on the fiber morphology. When the voltage increased from 10 kV to 18 kV, the SnSb-C fibers became more uniform and thicker with an average diameter of (150 ± 50 nm). The feed rate was also observed to affect the morphology of the fibers. Slight improvement in fibers profile was observed when feed rate decreased from 0.8 ml/h to 0.5 ml/h. Bead-free SnSb-C fibers with variable diameters were observed when 18 kV was applied between the needle tip and the collecting electrode as shown in the Figure 4. In general by varying voltage and feed rate, (Table 1) the formation of beads could be controlled on the nanofibers and diameter of the nanofibers (Figure 3). The SEM image as in Figure 3(f) of the SnSb-C composite nanofibers arises as a result of the most optimized electrospinning parameters. The average diameter was measured to be (≈ 100) nm as shown in Figure 4.

Table 1: SnSb-C nanofibers obtained under varying electrospinning conditions.

SEM image	Voltage (kV)	Working Distance (cm)	feed rate (ml/h)
(a)	10	15	0.8
(b)	15	15	0.8
(c)	15	15	0.7
(d)	16	15	0.7
(e)	16	15	0.5

(f)	18	15	0.5

[0079] To provide further insight into the morphology and structure on the resulting SnSb-C nanofibers, TEM investigations were carried out. The TEM images confirmed that the SnSb alloy particles were well-coated by the hollow carbon fibers and only a minor fraction of SnSb nanoparticles were attached on the surface of carbon nanofibers. The nanoparticles of SnSb encapsulated inside the carbon fibers were well dispersed. This was well evident from the micrographs, as shown in Figure 5, which showed SnSb nanoparticles confined inside the channels of the carbon fibers and in contact with the walls of the fibers. Only a minor fraction of SnSb particles resided outside the channels. The pseudo one-dimensional configuration of the SnSb inside the hollow carbon fibers is beneficial as it would provide easy and fast transport of electrons and lithium ions from the liquid electrolyte. Additionally, the residence of the SnSb at an optimum distance allows nullification of detrimental effects associated with the large volume changes occurring during reversible alloying and de-alloying reactions of Li with Sn. As an extra benefit, Sn nanoparticles appeared well embedded inside the carbon matrix, thus determining a protection against tin oxidation by air during the electrode fabrication.

[0080] Raman spectroscopy is another powerful tool to investigate microstructures. Figure 6 shows the Raman Spectrum of electrospun fibers after the heat treatment. The Raman spectra of carbonaceous materials have two characteristic bands including (1) ‘‘D-band’’, centered at the wavenumber of 1360 $cm^{-1}$and (2) ‘‘G-band’’, centered at the wavenumber of 1600 $cm^{-1.}$ The Carbon fibers are sp^2 conjugated carbon structure. The dehydration process and the amount of carbon content in SnSb-C fibers were investigated by Thermogravimetric Analysis (TGA) as depicted in Figure 7. TGA plot shows one step dehydration process in SnSb-C fibers

corresponding to a weight loss of 4% between 30-200^{o} C. This weight loss is attributed to the physisorbed water on the SnSb-C surface. The weight loss between 200-550 ^{o}C is due to the decomposition of the carbon and was estimated to be approximately 56 wt% of the total weight.

Example 3

Functional Characterization of SnSb-C Fibers

[0081] To investigate the electrochemical properties of porous Sb-C, Sn-C and SnSb-C fiber composite electrodes, cyclic voltammetry and galvanostatic charge-discharge cycling was performed. Figure 8 shows the cyclic voltammograms for first 5 cycles of the porous Sb-C, Sn-C and SnSb-C fiber composite electrodes. The Sb-C [Figure 8 (a)] exhibits a potential plateau at 0.25 V during the first discharge cycle which can be assigned to the formation of Li_xSb alloys. The irreversible peak at 1.3 V is attributed to the formation of solid electrolyte interphase (SEI) layer on the carbon surface as a result of the reductive decomposition of the electrolyte, which also contributes to the irreversible capacity loss during the first cycle. The first charge cycle peak at 1.1 V can be assigned to the de-alloying reaction of Li_xSb. From second cycle onwards, only peaks at 0.69 V and 1.1 V during alloying/de-alloying reaction were observed. This is the characteristic behavior of lithium insertion and deinsertion process of Sb. In the case of the Sn-C electrode [Figure 8 (b))] two reduction peaks at 0.52 V and 0.2 V in the first discharge cycle were observed and assigned to the alloying reaction between lithium and tin forming Li_xSn alloys. The very broad peak around 1.2 V is assigned to the formation of solid electrolyte interphase (SEI) layer on the carbon surface. The oxidation peaks at 0.5 V and 0.7 V in the first charge cycle can be assigned to the de-alloying reaction of Li_xSn. For the SnSb-C composites [Figure 8 (c)], a broad reduction peak appeared at 1.4 V in the first scan (alloying) which disappeared in reversed anodic scan and thereafter. This corresponded to the formation of the

solid electrolyte interphase (SEI) layer on the carbon surface. It can also be clearly seen that there are two pairs of redox peaks which appeared in the first cycle, corresponding to Li-Sb and Li–Sn alloying/de-alloying reactions. For SnSb-C composites, at the first Li_xSnSb phase form which then reacts with more Li^+ ions to produce Li_3Sb in the highly ductile Sn matrix.

[0082] This helps in relieving the mechanical strain associated with the expansion of the lattice during the formation of Li_3Sb. Following this, the lithium alloys with Sn. In addition, the lithium insertion into carbon may occur in the low voltage region around 0.1 V. These are indicated by the strong reduction peak ranging from 0.8 to 0.1 V. The reactions are summarized as follows:

$$SnSb + x\ Li^+ + xe^- \leftrightarrow Li_xSnSb\ (0 < x < 1.6) \quad (1)$$

$$Li_xSnSb + 1.4Li^+ + 1.4e^- \leftrightarrow Li_3Sb + Sn \quad (2)$$

$$Sn + 4.4Li^+ + 4.4e^- \leftrightarrow Li_{4.4}Sn \quad (3)$$

$$yC + zLi^+ + ze^- \leftrightarrow Li_zC_y \quad (4)$$

During delithiation, the reaction sequence is reversed and SnSb is restored. The shoulders observed at 0.2 V are assigned to the extraction of lithium ions from the carbon. The de-alloying of Sn occurs between 0.4 and 0.8 V, followed by Sb around 1.1 V. The ternary Li_xSnSb phase is then de-alloyed at > 1.2 V and SnSb is restored. The restoration of SnSb is beneficial in retarding the rate of agglomeration of Sn into larger grains which has been identified as one of the key reasons for poor cycle stability of Sn-based materials. The strong intense peaks in subsequent cycles indicate excellent electrochemical reversibility of the SnSb-C composite.

[0083] To study the cyclability at varying currents against lithium, Sb-C, Sn-C and SnSb-C fiber composite were cycled against lithium in half-cell configuration in the potential range 0.05–2.0 V (versus $Li^+|Li$). The voltage profiles of the SnSb-C nanocomposite electrode in the potential range of 0.05–2.0 V at a current density of 0.2 A g^{-1} is shown in Figure 9. The observed voltage

plateaus are in good agreement with the CV(Cyclic Voltammetry). An initial discharge (Li insertion) and charge (Li extraction) capacities for the porous SnSb-C nanocomposite electrode were 830 mAh g^{-1} and 658 mAh g^{-1}, respectively, with an initial Coulombic efficiency of 70%. This Coulombic efficiency is comparatively higher than those obtained for SnSb composite of previous works. In the second cycle the discharge and charge capacity of 647 and 637 mAh g^{-1} were obtained with Coulombic efficiency of 98.4%. A high reversible discharge capacity of 580 mAh g^{-1} is achieved during the 50^{th} cycle with a Coulombic efficiency of ~ 100%.

[0084] Figure 10 shows the specific capacity versus cycle number for Sb-C, Sn-C and SnSb-C composite at a current density of 0.2 A g^{-1}. After 50 cycles, the discharge capacities of Sb-C, Sn-C and SnSb-C are 300, 365 and 580 mAh g^{-1} respectively. This corresponds to capacity retention of 69% (Sb-C), 52% (Sn-C) and 90% (SnSb-C) with respect to the second discharge capacity. For SnSb-C composite even after 100 cycles the specific capacity is 580 mAh g^{-1}. The exceptional cyclability arises from a combination of factors related to the geometric configuration of SnSb alloy nanoparticles inside the carbon fiber morphology. The carbon (fibers) shell coated on the surface of SnSb nanoparticles offers adequate void space, which acts as a "buffer zone" to accommodate the large volume changes during alloying/de-alloying processes and it prevents the particles from aggregation, leading to alleviation of the pulverization after long time cycling. The SnSb nanoparticles encapsulated in carbon fibers provide good specific surface area, which improves the electrical contact as well as lithium ion conduction. In addition, the entire fabrication procedure is straightforward with reasonably good yield. The diameter and thickness of carbon fibers can be readily tuned by adjusting the electrospinning parameters. The capacity values for the SnSb-C are much higher compared to those for SnSb-C composite nanomaterials reported in the prior art.

[0085] The SnSb-C showed very good rate capability (Figure 11) in the current range (0.2-5) A g^{-1}. The specific discharge capacities are respectively 830, 444, 363, 286 and 210 mAh g^{-1} at 0.2, 0.5, 1, 3 and 5 A g^{-1}. The rate performance at such high current densities is better than other SnSb-C composite anodes previously reported in literature. Furthermore, initial capacity values could be recovered when the testing current is reverted back to the initial low current density (= 0.2 A g^{-1}). The enhanced rate capability of the SnSb-C is attributed to the combined effects of homogenous distribution of SnSb nanoparticles inside the carbon fiber morphology. The nanometer size significantly increases the rate of Li^+ insertion/extraction because of the short diffusion length for lithium-ion transport within the particles, enhancing the rate capability and power density. The same is also true for electron transport, which is also enhanced in nanomaterials. In addition, good specific surface area ensures high electrode–electrolyte contact area which improves significantly the lithium-ion flux (transport for electrons and lithium ions). The SnSb nanoparticles encapsulated inside porous carbon are mechanically stable and absorb the undesirable volume changes occurring during successive cycling. The carbon fiber also provides percolating electron pathways between the SnSb particles. Finally, the strain associated with insertion/extraction is often better accommodated, avoiding destruction of the material structure and improving the life cycle of the cell.

[0086] The improvement in electrochemical properties was further investigated by electrochemical impedance spectroscopy. Impedance spectra were collected before and after 50 cycles. The semicircle at high frequencies is likely to be due to lithium-ion migration in the surface layer (SEI film) of electrode, while the semi-circle at medium frequencies is usually assigned to the charge transfer process. The line at low frequencies is ascribed to the diffusion of the lithium ions in the active material. Figure 12 .1 reveals that both the SEI film resistance and

the charge transfer resistance decrease with increasing cycle number. The decreasing SEI film resistance could be attributed to the result from the pulverization of SnSb particles where some new surface will be formed and thus new SEI film, which will result in low impedance. The decrease in charge transfer resistance (R_{ct}) reflects the increase in active surface area caused by pulverization of SnSb-C and local break-up of SEI film. An equivalent circuit model was constructed to analyze the impedance spectra as shown in Figure 12.2 where R_e is the resistance of the electrolyte or uncompensated resistance between the working electrode and the lithium reference electrode,CPE1 -the constant phase element (or capacitance) of the SEI layer ,R_f - the migration of the Li^+ ions through the SEI film,CPE2 - capacitance of the double layer (Q_{dl}) on the particle surface, R_{ct} - charge-transfer impedance (R_{ct}) on electrode/electrolyte interface or the resistance of the SEI layer and Z_w is the diffusion of the Li^+ ions in the bulk of the electrode.

FOR Indian Institute of Science

Tarun Khurana [IN/PA-1325]
Dated: 8th Oct' 14

CLAIMS

We claim:

1. An integrated method for synthesis of Sn-alloy nanoparticle assembly embedded inside one dimensional porous carbon nanofibres comprising the steps of:

   (a) electrospinning a precursor to produce nanofibres, the precursor comprising of a polymer and Sn-X compositions; and

   (b) heat sintering and carbonization of the nanofibres to obtain the Sn-alloy nanoparticles assembly embedded inside carbon nanofibers;

   wherein,

   X is an element and the molar composition of Sn and the element is 1:1; and

   the Sn-alloy nanoparticle assembly embedded inside one dimensional porous carbon nanofibres acts as an electrode.

2. The integrated method according to claim 1, wherein the polymer is selected from the group consisting of polyacrylonitrile (PAN), polyvinyl alcohol (PVA), polyethylene oxide (PEO), and polyvinyl pyridine (PVP), and poly(methyl)methacrylate (PMMA).

3. The integrated method according to claim 1, wherein the element is selected from the group consisting of antimony (Sb), cobalt (Co), iron (Fe), Ge (germanium), nickel (Ni), copper (Cu) or the combination thereof.

4. The integrated method of claim 1, wherein an interparticle distance inside Sn-alloy nanoparticles ranges from 10 to 30 nm and an interparticle distance in contact with carbon fibers is 150 ± 50 nm.

5. The integrated method of claim 1, wherein the Sn-alloy nanoparticle assembly embedded inside one dimensional porous carbon nanofibres acts as an anode in battery chemistries comprising lithium, sodium, and metal-air systems..
6. The integrated method of claim 1, wherein said method does not require use of carbon additives.
7. The integrated method of claim 1, wherein no additives are required to be added to a liquid electrolyte for establishment of a stable electrode-electrolyte interface.
8. A secondary battery using the Sn-alloy nanoparticle assembly embedded inside one dimensional porous carbon nanofibres as an electrode, prepared by the integrated method according to claim 1, wherein the secondary battery is selected from the group consisting of lithium, sodium, and metal air systems.

FOR Indian Institute of Science

Tarun Khurana [IN/PA-1325]
Dated: 8th Oct' 14

ABSTRACT

SN-ALLOY NANOPARTICLE CARBON ONE-DIMENSIONAL ASSEMBLIES FOR RECHARGEABLE BATTERIES

An integrated method for synthesis of Sn-alloy nanoparticle assembly embedded inside one-dimensional porous carbon nanostructures such as carbon fibers, using an electrochemical technique coupled with an optimized heat sintering protocol is disclosed in the present invention. The Sn-alloy nanoparticle assembly arranged inside one-dimensional porous carbon structures is used as an electrode system in secondary batteries, particularly as an anode in various battery chemistries such as lithium, sodium, metal-air systems, and the like.

FOR Indian Institute of Science

Tarun Khurana [IN/PA-1325]

Dated: 8th Oct' 14

Fig. 1

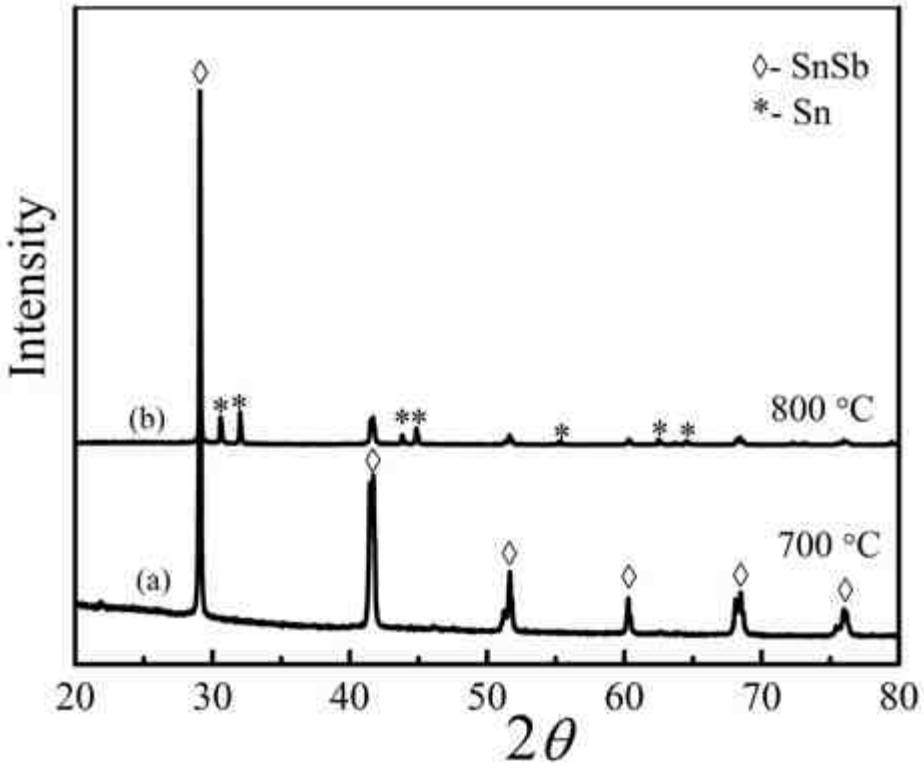
◊- SnSb
*- Sn
Intensity
(b)
800 °C
(a)
700 °C
20
30
40
50
60
70
80
2θ

Fig. 2

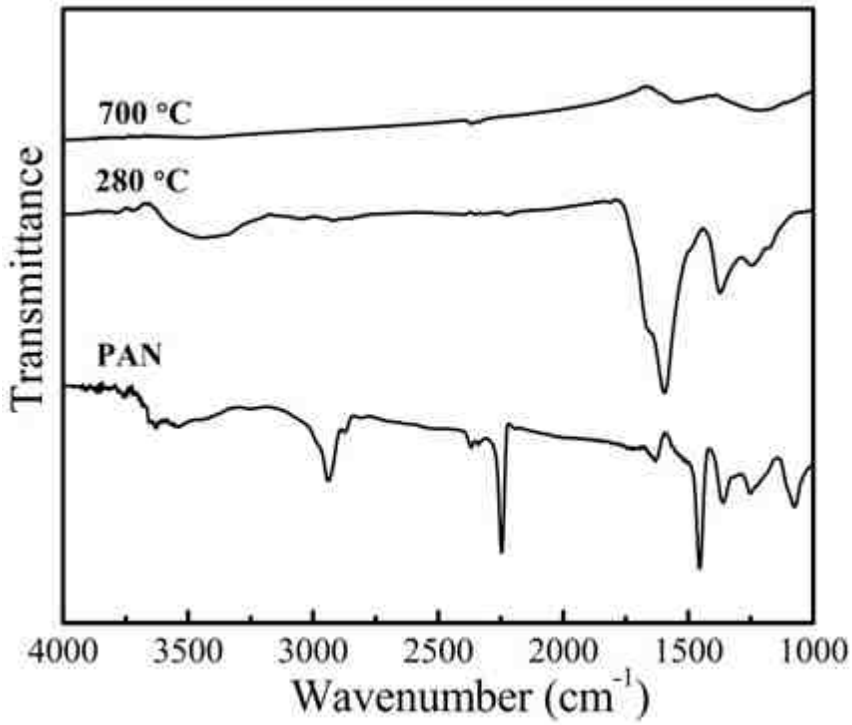
700 °C
280 °C
PAN
Transmittance
4000
3500
3000
2500
2000
1500
1000
Wavenumber (cm-1)

Fig. 3

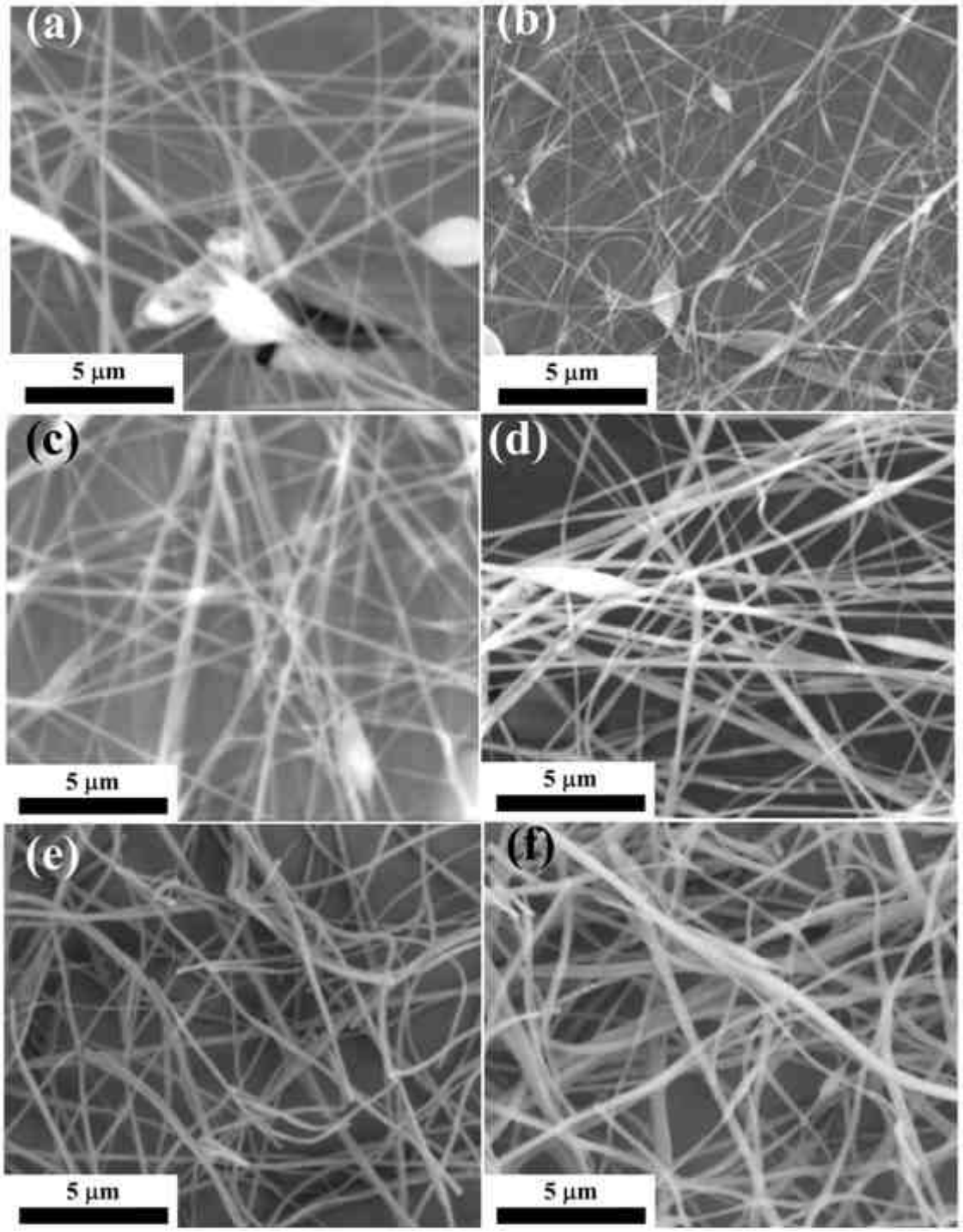

Fig. 4

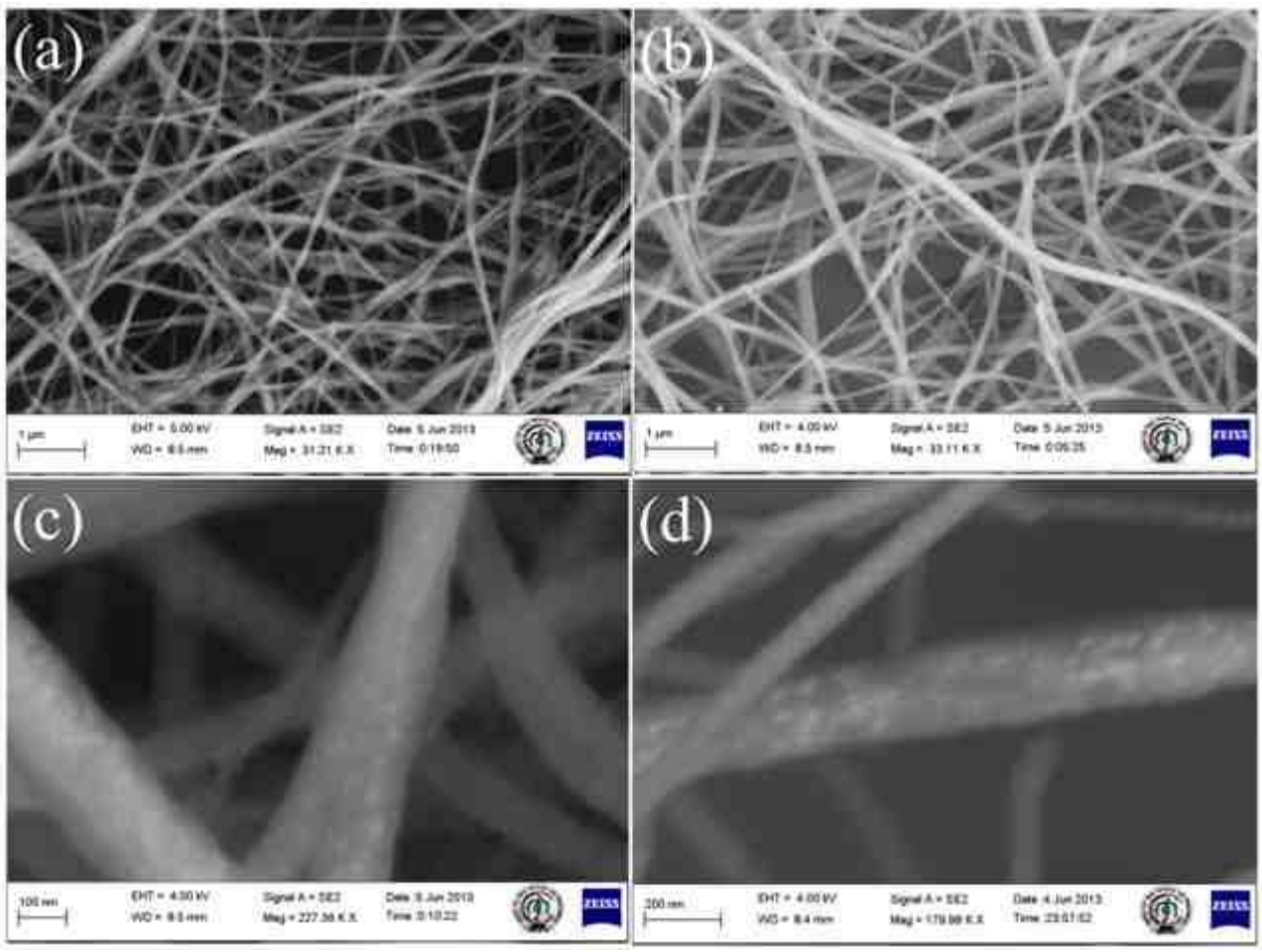

Tarun Khurana
Regd. Patent Agent [INPA-1325]
Dated: 8th October, 2014

Fig. 5

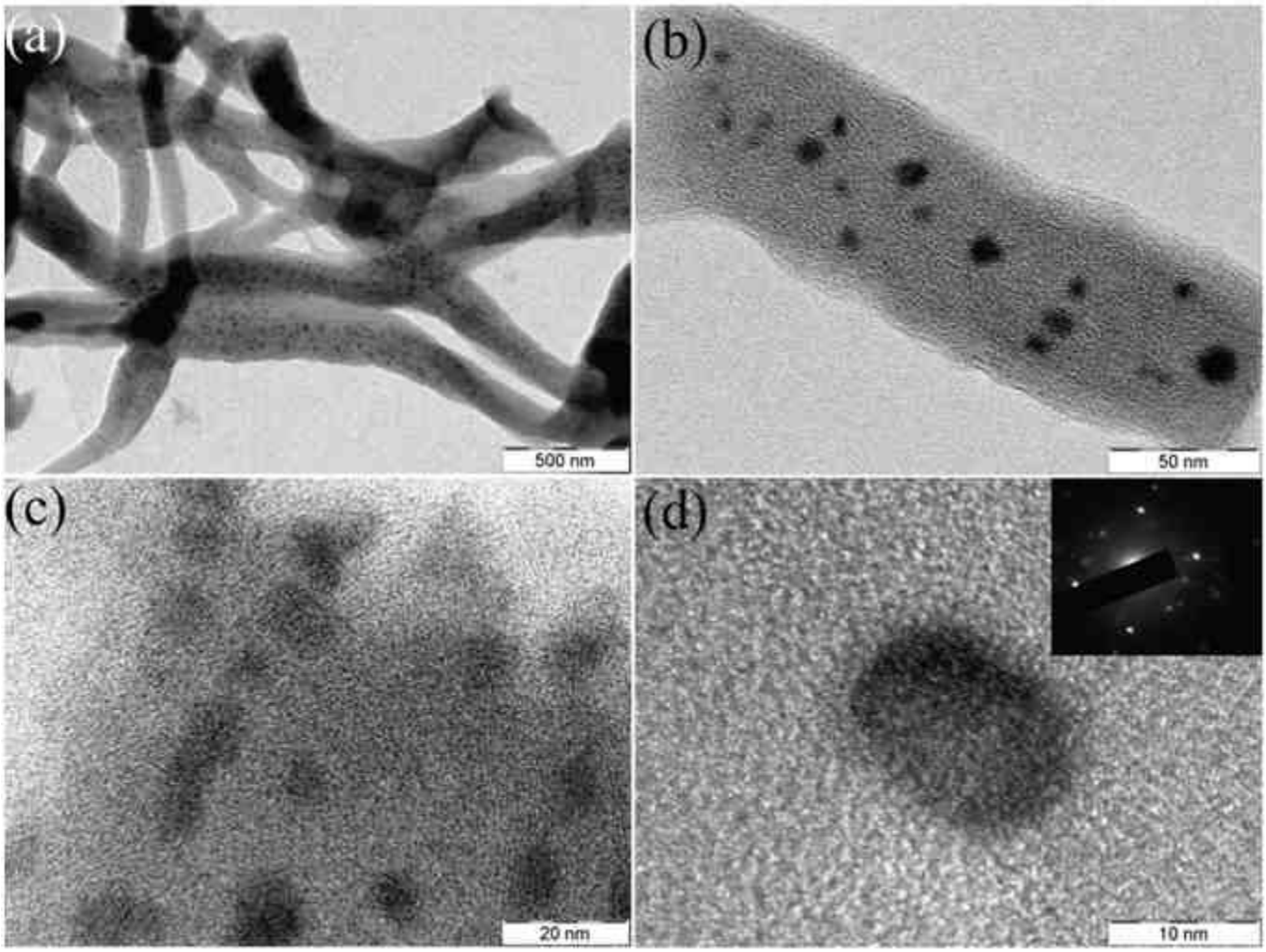

Fig. 6

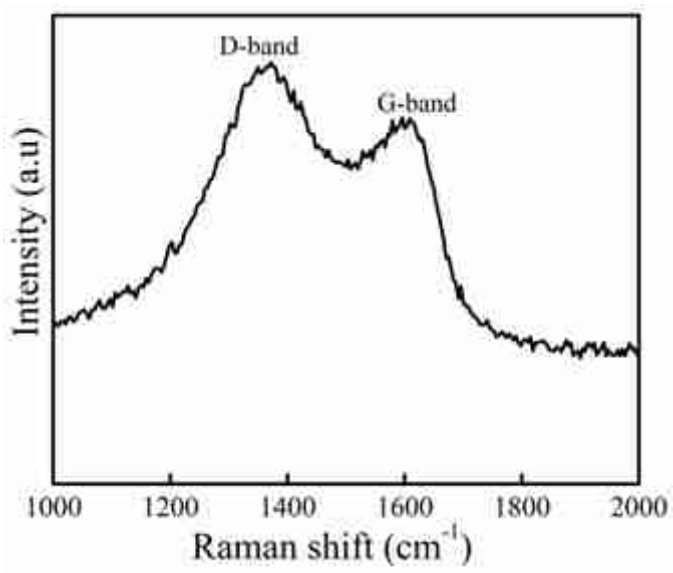
D-band
G-band
Intensity (a.u)
1000
1200
1400
1600
1800
2000
Raman shift (cm-1)

Fig. 7

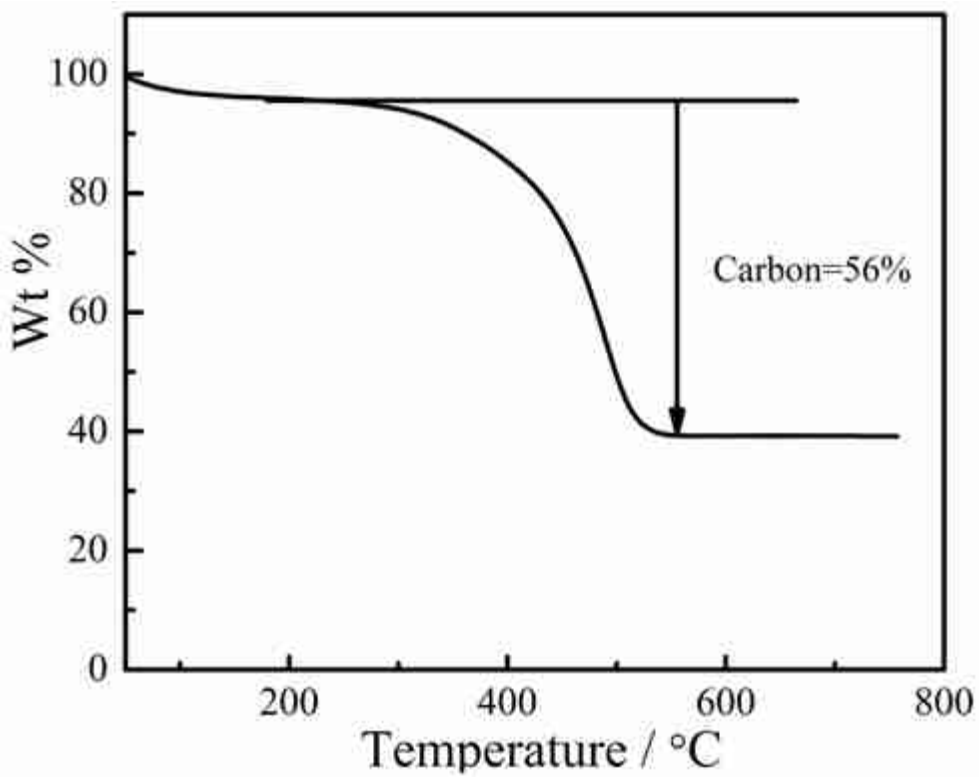
100
80
60
40
20
0
Wt %
Carbon=56%
200
400
600
800
Temperature / °C

Fig. 8

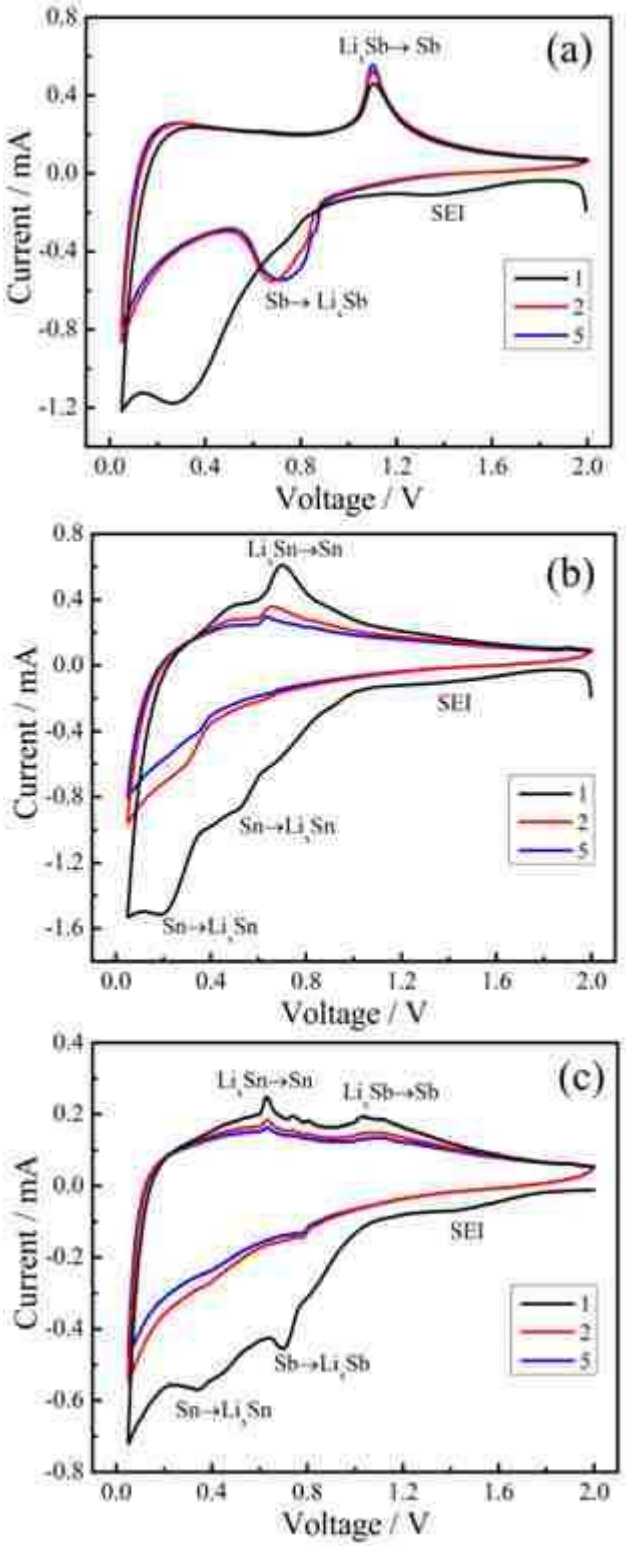
(a)
Li3Sb→ Sb
SEI
Sb→ Li3Sb
1
2
5
Current / mA
Voltage / V
(b)
Li4Sn→Sn
SEI
Sn→Li2Sn
Sn→Li7Sn
1
2
5
Current / mA
Voltage / V
(c)
Li4Sn→Sn
Li3Sb→Sb
SEI
Sb→Li3Sb
Sn→Li2Sn
1
2
5
Current / mA
Voltage / V

Fig. 9

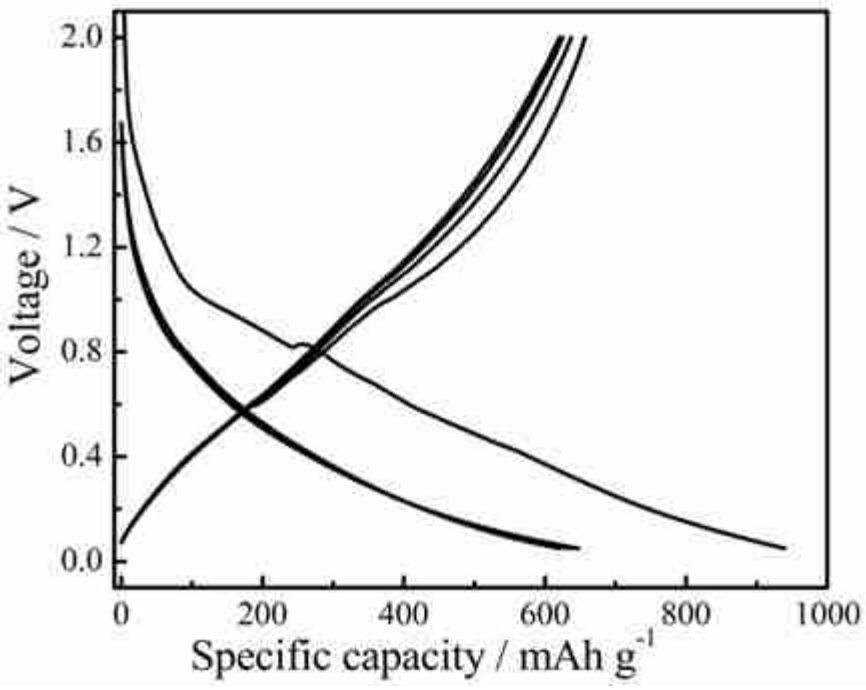
Voltage / V
2.0
1.6
1.2
0.8
0.4
0.0
0
200
400
600
800
1000
Specific capacity / mAh g-1

Fig. 10

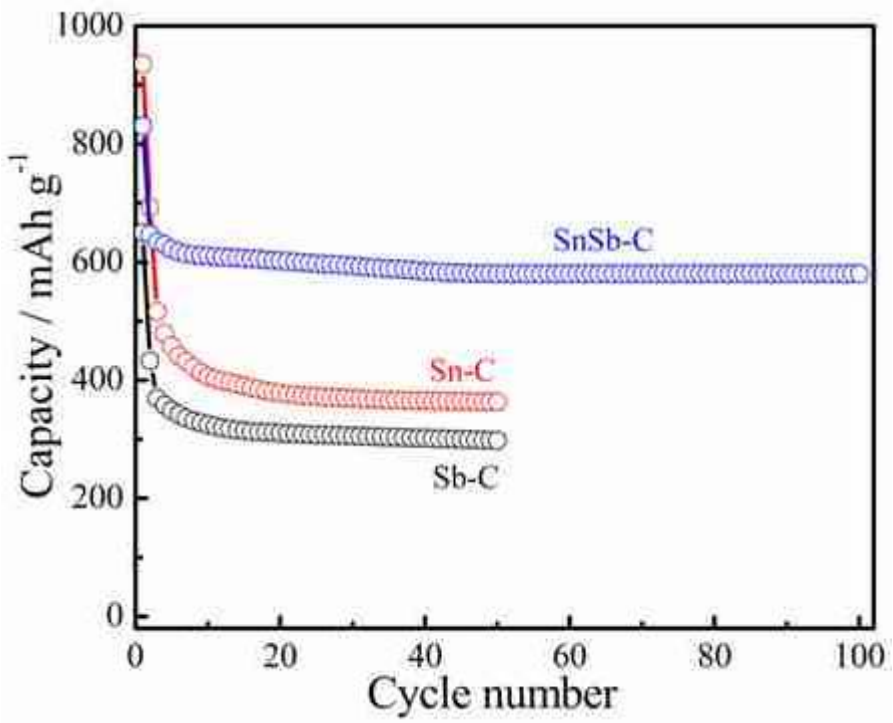
Capacity / mAh g-1
1000
800
600
400
200
0
0
20
40
60
80
100
Cycle number
SnSb-C
Sn-C
Sb-C

Fig. 11

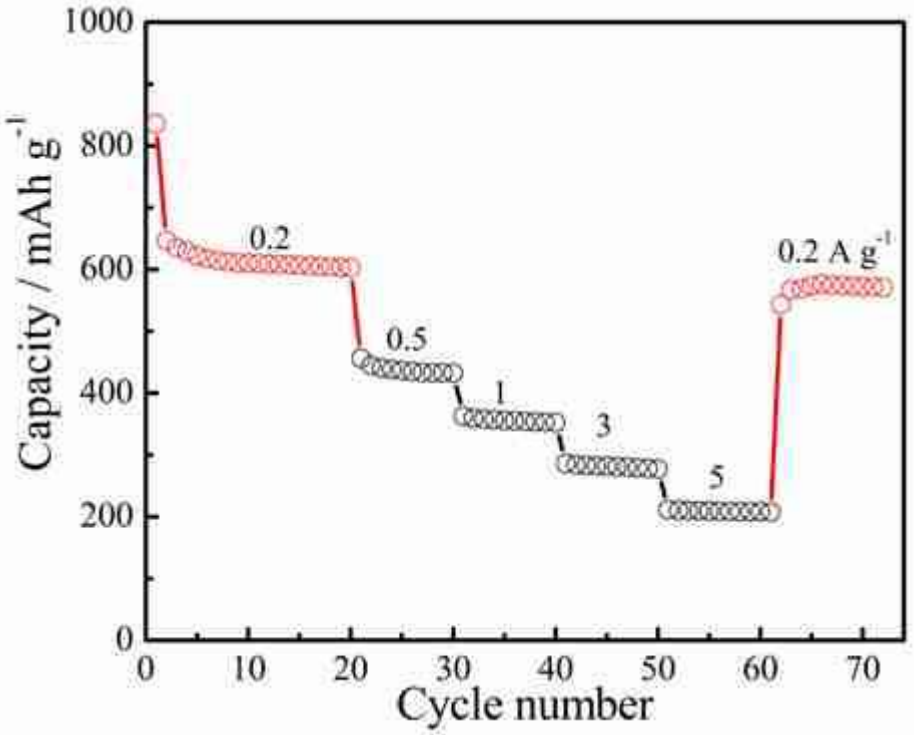

Fig. 12

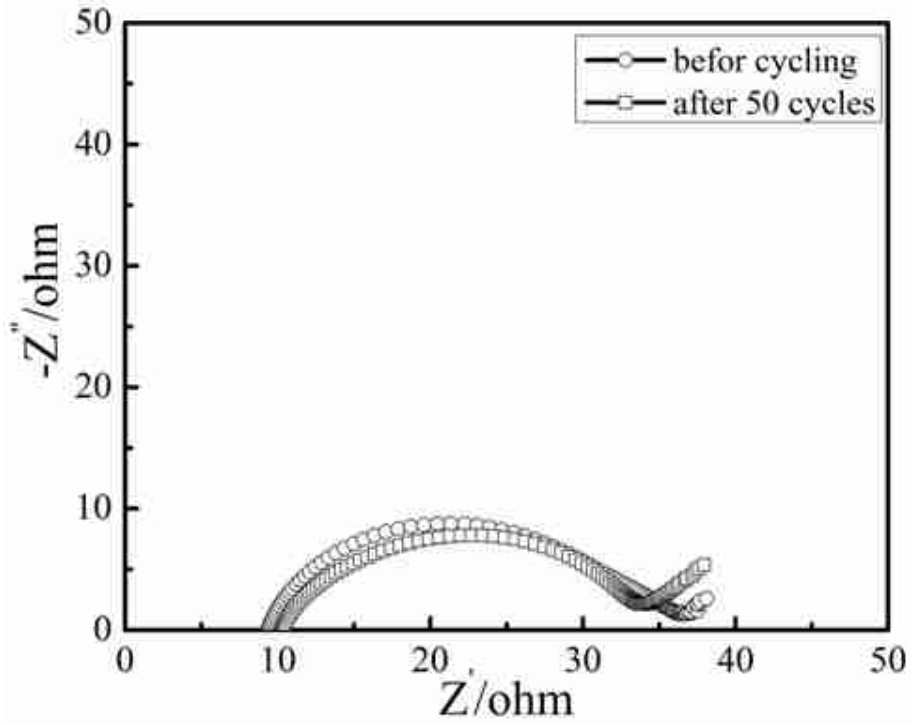

Tarun Khurana
Regd. Patent Agent [INPA-1325]
Dated: 8th October, 2014